Reduction of the electron thermal conductivity produced by ion Bernstein waves on the Frascati Tokamak Upgrade tokamak

R. Cesario, A. Cardinali, C. Castaldo, M. Leigheb, M. Marinucci, V. Pericoli-Ridolfini, F. Zonca, G. Apruzzese, M. Borra, R. De Angelis, E. Giovannozzi, L. Gabellieri, H. Kroegler, G. Mazzitelli, P. Micozzi, L. Panaccione, P. Papitto, S. Podda, G. Ravera, B. Angelini, M. L. Apicella, E. Barbato, L. Bertalot, A. Bertocchi, G. Buceti, S. Cascino,[a] C. Centioli, P. Chuilon, S. Ciattaglia, V. Cocilovo, F. Crisanti, F. De Marco, B. Esposito, G. Gatti, C. Gormezano, M. Grolli, F. Iannone, G. Maddaluno, G. Monari, P. Orsitto, D. Pacella, M. Panella, L. Pieroni, G. B. Righetti, F. Romanelli, E. Sternini, N. Tartoni, P. Trevisanutto,[a] A. A. Tuccillo, O. Tudisco, V. Vitale, G. Vlad, and M. Zerbini

Associazione EURATOM-ENEA sulla Fusione, Centro Ricerche Frascati, C.P. 65, 00044 Frascati, Rome, Italy

(Received 19 March 2001; accepted 19 July 2001)

Operating with a high frequency and a wave guide antenna, the ion Bernstein wave (IBW) experiment on the Frascati Tokamak Upgrade is not dominated, as expected, by nonlinear plasma edge phenomena. By coupling IBW power, a simultaneous increase of plasma density and central electron temperature ($\geqslant 2$ keV) is produced when the confinement magnetic field is adjusted to set an ion cyclotron resonant layer in the plasma bulk. Transport analysis indicates a reduction of the electron thermal transport inside the internal resonant layer larger than a factor of 2. © *2001 American Institute of Physics.* [DOI: 10.1063/1.1408912]

Coupling of ion Bernstein waves (IBW) to tokamak plasma by mode conversion of the lower hybrid wave (LHW) was proposed as a technique to suppress turbulence with sheared flow in advanced tokamaks.[1] Although operating in similar conditions, not all the IBW experiments carried out so far achieved successful results in plasma heating and improving transport.[2–7] The not conclusive evidence on IBW scheme validity was attributed to nonlinear plasma edge phenomena affecting antenna coupling, producing parametric instabilities, impurity influx and causing poor IBW power penetration in the bulk.[4,8–10]

The distinctive features of the IBW experiment on the Frascati Tokamak Upgrade (FTU) are the high frequency, $f_0 = 433$ MHz, and the wave guide antenna, which are expected to reduce the aforementioned parasitic effects.[1,9–11] As observed in the experiment, the plasma density at the edge was not reduced by the ponderomotive effect, and the antenna coupling exhibited a linear behavior when IBW power was increased up to the maximum value available from radio frequency (rf) generator (0.45 MW).[12] As a consequence, plasma inhomogeneity-induced convective losses can inhibit parametric instability.[8,13]

According to the linear theory, in FTU, the launched LHW mode converts into IBW at the cold LH resonant layer, which is located in the scrape-off (SOL) (at $n_e \approx 4 \times 10^{18}\,\mathrm{m}^{-3}$, hydrogen plasma).[13,14] In the IBW-FTU experiments, the standard plasma target is optimized to have good core absorption by operating with a hydrogen plasma with (resonant) toroidal field $B_T = 7.9$ T, which locates the 4th Ω_H, the only ion-cyclotron harmonic layer in the machine, at about a third of the minor radius in the low field side. Full deposition at the first pass of the rf power on the plasma electrons and ions is expected to occur up to the resonant layer. An indirect evidence of the IBW propagation in the bulk can be obtained by a plasma target with similar parameters, but with $B_T = 5.9$ T (nonresonant field). In this case a complete rf power absorption in the plasma periphery is expected, due to location of the 6th Ω_H harmonic resonant layer at the plasma edge. To obtain clearer results, magnetohydrodynamic (MHD) quiescent targets are chosen in all the cases by operating with low enough plasma current, $I_p = 0.25$–0.35 MA, corresponding to an edge safety factor $q_{\mathrm{edge}} \approx 10$. Moreover, the ohmic (OH) power is comparable with IBW power, which allows a better assessment of direct rf heating of plasma particles. The line averaged plasma density is $n_e / n_{\mathrm{Greenwald}} \approx 0.25$ and the plasma column located a few centimeters away from the toroidal limiter, leaned on the poloidal limiter. This operating condition allows the minimization of the impurity release from the walls eventually caused by rf-induced turbulence in the SOL.

A very low activity of parametric instability (with sideband >60 dB below pump wave power) is observed by standard rf probe set up.[8] Parametric instability, being a typical phenomenon observed during the LH heating experiments, shows that the wave guide antenna works properly in launching the LH wave, necessary for IBW coupling. On the other hand, the low intensity of this phenomenon indicates that the wave interaction with the edge plasma is small and should not prevent the wave propagation into the plasma core as occurred, instead, in Doublet III-D.[4]

The results obtained injecting $P_{\mathrm{IBW}} = 0.25$ MW of coupled rf power at resonant and nonresonant magnetic

[a]ENEA Guest.

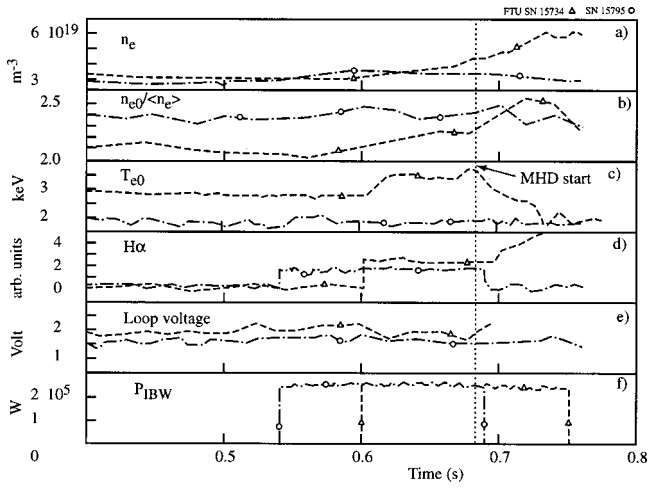

FIG. 1. Comparison of the time evolution of the main plasma parameters during injection of the same IBW power (0.25 MW), in plasma shots with resonant magnetic field: $B_T=7.9$ T ($I_P=330$ kA) (triangles), and with $B_T=5.9$ T ($I_P=240$ kA) (circles). Line averaged plasma density (a), density profile peaking $n_{e0}/\langle n_e\rangle$ (b), central electron temperature from ECE (c), $H\alpha$ emission from the outer plasma edge (d), loop voltage (e), IBW power (e).

fields are compared in Fig. 1. For $B_T=7.9$ T, an increase of n_e from 3 to 5×10^{19} m^{-3} is observed [Fig. 1(a)] together with a substantial peking of the density radial profile, $n_{e0}/\langle n_e\rangle$ [Fig. 1(b)]. For $P_{IBW}=0.35$ MW, a similar amount of density rise is obtained, but with a further increase of the density profile peaking (50%). For $B_T=5.9$ T instead, only a much lower density rise (20%) is observed, not accompanied by a change of the density peaking profile. An increase of the central electron temperature T_{e0} by about 1 keV [Fig. 1(c)], together with peaked $T_e(r)$ and soft x-rays emission profiles are only observed at the resonant magnetic field. After 90 ms, the onset of a MHD mode ($n=1$, $m=2$) depresses immediately T_{e0}, accordingly to data from soft x-ray tomography. A few milliseconds later, the pressure profile peaking begins to decrease. So far, the MHD activity can only be delayed by about 100 ms, and appears to be the main cause for the termination of the IBW related effects. To be noted is that all the central channels of the ECE polychromator (not presented here), sampled at 20 kHz rate, showed a temperature rise in the plasma core with a 4 ms delay from the rf switch-on time, starting with a zero time derivative. This would indicate that no direct heating of central electrons takes place (not expected, however, by the plasma wave theory). Indeed, in typical experiments of electron cyclotron radio frequency heating, a few hundred kW ECRH power produce a central direct electron heating in FTU. The central ECE polychromator signal shows a prompt temperature rise (rise time<1 ms) in the plasma core at the rf switch-on. The central temperature increases with a very steep time derivative related to the rf heating power. Conversely, the T_{e0} rise during IBW coupling cannot be related to direct central electron heating by the radiofrequency power, but it can be due to a change in the heat transport properties (see below). A central ion temperature $T_{i0}=1.8\pm0.2$ keV is measured by He-like iron spectroscopy; by coupling 0.3 MW IBW power, about 0.2 keV temperature increase is typically produced when operating at the resonant magnetic field.

All discharges with IBW exhibit a similar rf interaction with the edge plasma, as suggested by the similar values of P_{rad}/P_{tot} which are in both cases 65% in the OH phase and 75% during the rf pulse. The H_α emission from the outer edge shows a sharp increase after the rf is switched-on [Fig. 1(d)]. After a similar rf-induced increase of the emission from the toroidal limiter, a decrease occurs only operating at the resonant magnetic field, when the peaking of the density profile develops. Finally, the loop voltage [Fig. 1(e)] does not show a significant change during the rf power injection, before the occurrence of the MHD activity. Bremsstrahlung central emission measurements give a $Z_{eff}\approx3.5$ in the OH phase, which decreases appreciably during rf injection. Such a value is not unusual in FTU for the operating plasma densities of the examined discharges, and it is due to the metallic FTU first wall.[15] However, these operating conditions should not prevent the IBW propagation in the bulk.

The oxygen concentration was estimated to increase during IBW injection from 0.5% to about 1%, accordingly to ultraviolet (UV) spectral analysis, due to a probable desorption from the metallic wall, induced by the impact of ions accelerated by nonlinear plasma wave interactions in the SOL.[9] This impurity influx is estimated to produce only a small fraction (15%) of the density rise observed during the rf injection in the discharges with resonant magnetic field; an equivalent contribution to the density rise is expected from the H_α increase. The rest of the density rise can only be explained by an increase of the particle confinement.

In performing the experiment, care was spent to reduce the effect of the impurity influx. In FTU, an acceptable level of oxygen release is attained by letting the plasma lean on the poloidal inconel limiter; this effect is probably due to both the smaller wetted surface and the nature itself of the first wall material. During the IBW pulse, the bolometric losses P_{rad} evolve from a centrally peaked to a hollow profile, with the maximum of the emission at 15 cm from the center. Bremsstrahlung emission gives an appreciable reduction of Z_{eff}, inside this region, and an increase outside. These results are consistent with the estimated density variation. An increase a factor of 2 for oxygen and a decrease a factor of 3 for molybdenum, respectively, is observed with oxygen and molybdenum being the dominant heavy and light impurities. These effects are also consistent with an off-axis accumulation of heavy impurities, outside of the region delimited by the ion cyclotron resonant layer, due to quasi-linear effects occurring in the IBW propagation region, as predicted in Ref. 16.

Typical plasma density and electron temperature profiles are presented in Fig. 2, as obtained by coupling different amounts of IBW power up to $P_{IBW}\approx0.35$ MW, the maximum available coupled power. The electron temperature increases by about 1 keV with 0.25 MW [Fig. 2(a)] and by about 2 keV with 0.3 MW [Fig. 2(b)] and 0.35 MW [Fig. 2(c)]. A 200 eV drop of the temperature is observed at about 15 cm from the center, outside the resonance layer. This is attributed both to the increase of the density there (about 40%) and to the increased radiation losses due to the light impurity release. The increase of T_{e0}, which starts to appear

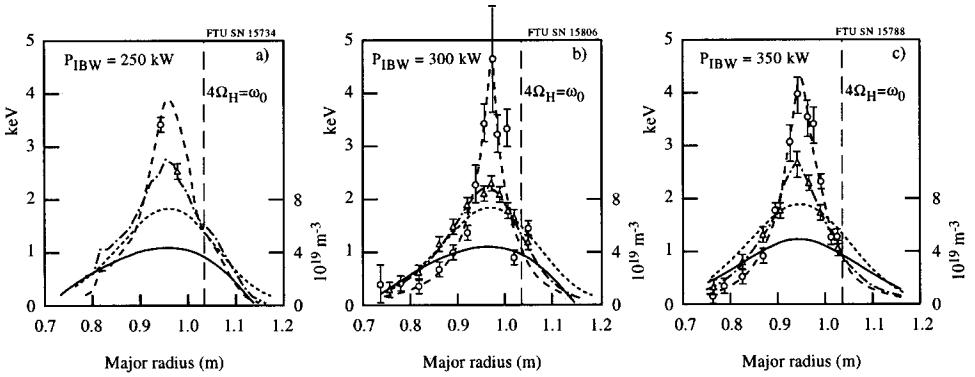

FIG. 2. Electron temperature (scale on left) and plasma density (scale on right) profiles during the phases: Ohmic (triangles and continuous curve, respectively) and with IBW (dots and dotted curve, respectively). Standard discharges with resonant B_T are considered. $P_{IBW}=0.25$ MW, $I_P\approx 0.33$ MA (experimental curves of ECE) (a); $P_{IBW}=0.30$ MW, $I_P\approx 0.30$ MA (dots and triangles are the experimental points of Thomson scattering) (b); $P_{IBW}=0.35$ MW, $I_P\approx 0.32$ MA (dots and triangles are the experimental points of Thomson scattering) (c). Note that in (b) the experimental point coincides with the plasma center. The different central temperature values in the ohmic phase can be attributed to differences of the operating plasma current.

in the experiment for $P_{IBW}\geqslant 0.1$ MW, seems to saturate at $P_{IBW}\approx 0.3$ MW.

Improved transport produced by cooling plasma edge was observed in some experiments.[17] Several tests have been performed to make evident a possible role of impurity in determining the IBW results. Neon (cooling rate similar to oxygen) was injected in FTU instead of rf power in plasma targets with resonant magnetic field. The neon puff (3% of the whole flux of gas) produced an increase of density (35%), but no peaking of the density profile was observed. Moreover, no appreciable change of the Z_{eff} profile occurred. Higher fluxes of the neon puff (up to 15% of the whole flux of gas) produced an increase of density ($\simeq$100%), loop voltage and Z_{eff}. Therefore, the IBW-FTU results cannot be related to impurity influx only.

Transport analysis was performed for IBW plasma shots to test if the observed effects could be explained in terms of a reduced central electron thermal diffusivity. The analysis was made using the JETTO code[18] in interpretative mode. In this mode, the profile of the electron thermal diffusivity, χ_e, are obtained by inputting: The profiles of plasma density, electron temperature, radiation, effective ion charge from experimental measures, the magnetic reconstructed equilibrium. The considered ion temperature profile, shown in Fig. 3, is calculated assuming neoclassical ion transport, typically exhibited at the considered FTU regime.[19] In the figure, the central ion temperature, measured before and during the IBW power injection, is shown. In order to test the influence of ion temperature on the χ_e evaluation, several analyses were performed assuming different ion temperature profiles, in which the central and the off-axis ($r/a\approx 1/2$) temperatures were changed within a wide range ($\approx$50%). As a result no significant change of χ_e was found. The ion temperature affects weakly the electron thermal diffusivity due to the low ion-electron thermal exchange, occurring at the considered low operating densities ($\langle n_e\rangle\approx 0.5\times 10^{20}\,\text{m}^{-3}$). Such small effect is consistent with the different values of the measured central ion and electron temperatures ($T_{e0}/T_{i0}\approx 2$).

The experimental loop voltage behavior was well reproduced, assuming a radially flat neoclassical plasma resistivity, consistent with the measured radially averaged $Z_{\text{eff}}=5\pm 1$. According to ray-tracing calculations, the rf power is assumed to be deposited with Gaussian profiles on plasma ions and electrons at plasma radii $R\geqslant R(4\Omega_H)$. Details of the shape of the deposition and of the Z_{eff} profile did not affect appreciably the transport analysis results.

The obtained χ_e profile is shown in Fig. 4. Here, the OH and IBW phases are compared for two cases with $P_{IBW}=0.25$ MW and 0.35 MW. A factor 2 drop of χ_e during the IBW phase in the internal plasma region for $R\leqslant 1.03$ m, for $P_{IBW}=0.25$ MW (a larger drop of χ_e is observed for $P_{IBW}=0.35$ MW) suggests that a transport barrier is formed. The experimental pressure profiles during the OH and the rf phases are also shown in the figure. During rf, the pressure starts to increase for $R\leqslant 1.02-1.05$ m, consistently with the calculation of turbulence suppression. The β during the OH phase is $\beta\approx 2\times 10^{-4}$ and 40% increase occurs during IBW injection. During the rf pulse the OH power profile stays constant within 10%. At the last analyzed time-frame, just before the MHD activity starts, the electric field is not yet

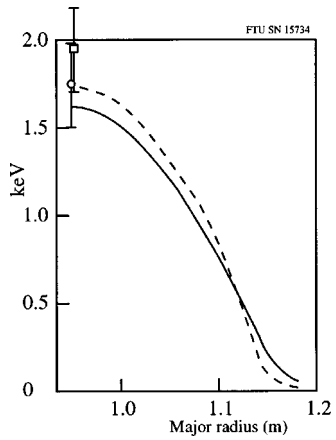

FIG. 3. Neoclassical ion temperature profile and central ion temperature obtained from He-like spectroscopy of iron spectroscopy, at different times: before (continuous curve and circle, respectively) and during IBW power injection (dashed curve and square, respectively).

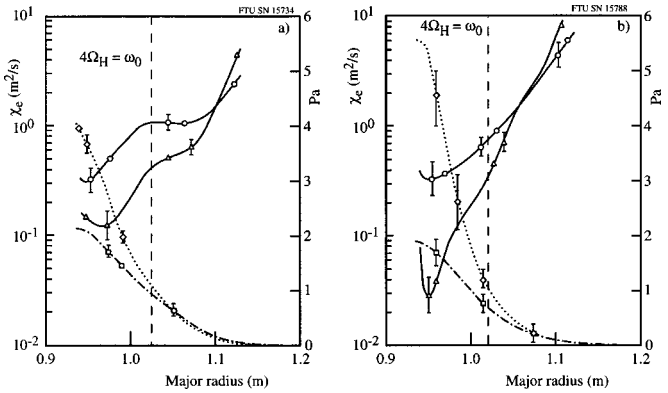

FIG. 4. Electron thermal diffusivity profile from transport analysis, before (circles) and during IBW injection (triangles), for coupled IBW power 0.25 MW (a) and 0.35 MW (b). The bars show the error produced by the experimental kinetic profiles and the effective ion charge. The respective measured pressure profiles are shown for comparison.

fully relaxed, and its central value drops with the plasma resistivity.

In order to provide further support to the argument that the central temperature rise was not caused by a direct IBW central electron heating, a predictive analysis producing the time evolution of the electron temperature profile by JETTO was performed, assuming χ_e unchanged with respect to the OH phase. As a result, an off-axis full deposition of the rf power will give only a small fraction of the observed T_{e0} increase. Instead, such increase is reproduced assuming an on axis IBW power deposition of 0.15 MW absorbed on the central electrons, but a prompt central temperature rise at the rf switch-on is obtained, with a very steep time derivative related to the assumed heating power. Conversely, in the experiment, the T_{e0} rise at the rf switch-on shows a markedly different behavior, with a flat slope derivative. In conclusion, transport analysis (interpretative) performed by inputting the experimental data shows a significant reduction of the electron thermal diffusivity in the core. Analogously, a time evolution of the electron temperature consistent with the experimental observations is simulated by (predictive) transport analysis only when assuming a significant reduction of the electron thermal diffusivity to the plasma core. The assumption of IBW power centrally deposited does not reproduce the time behavior of the measured electron temperature.

Operating in the same low-frequency range, the previous IBW experiments were dominated by nonlinear plasma phenomena at the edge, which in some cases inhibited improved confinement effect to be reproduced. As expected by combining the wave guide antenna and a high-operating frequency, during the IBW experiment on FTU no significant activity of the aforementioned phenomena and a low-impurity influx are observed. A simultaneous increase and peaking of plasma density and electron temperature is produced by IBW, as never observed in previous IBW experiments. Transport analysis shows that a significant χ_e reduction occurs in the plasma interior. A possible qualitative explanation is suggested as follows. Sheared plasma flows induced by IBW are expected to produce turbulence suppression in a thin region (width$\approx\rho_{\mathrm{Li}}$) located at the resonant layer,[20] which, in turn, could affect electron transport via electron temperature gradient modes. The core reduction of χ_e may be associated with different parameter regimes of micro-instability driven plasma dynamics, e.g., kinetic interchange modes and electromagnetic (Alfvén) drift waves (drift Alfvén–kinetic ballooning modes), determined by both plasma beta and alpha (ballooning) parameters. This topic needs further work to be assessed, and it is beyond the scope of the present work.

The experiments performed at different operating magnetic fields and by neon puffing ruled out that the improved confinement was produced by impurities. The FTU results provide robustness of the IBW concept, as necessary for utilizing it in advanced tokamaks.[21]

ACKNOWLEDGMENTS

The authors acknowledge F. Paoletti for the useful discussions and contributions to this work and L. M. Carlucci for technical/editorial comments.

[1] M. Ono, Phys. Fluids B **2**, 241 (1993), and references therein.
[2] M. Ono *et al.*, Phys. Rev. Lett. **60**, 294 (1988).
[3] J. D. Moody *et al.*, Phys. Rev. Lett. **60**, 298 (1988).
[4] R. Pinsker *et al.*, Nucl. Fusion **33**, 777 (1993), and references therein.
[5] J. C. Rogers *et al.*, in *Proceedings of the 12th Topical Conference on RF Power in Plasmas*, Savannah 1997 (AIP, New York, 1997), Vol. 403, p. 13.
[6] T. Seky *et al.*, Nucl. Fusion **32**, 2189 (1992).
[7] B. Le Blanc *et al.*, Phys. Plasmas **2**, 741 (1995); B. Le Blanc *et al.*, Phys. Rev. Lett. **82**, 331 (1999).
[8] R. Cesario *et al.*, Nucl. Fusion **34**, 261 (1994), and references therein.
[9] R. Cesario *et al.*, Nucl. Fusion **34**, 1527 (1994).
[10] D. A. Russel *et al.*, Phys. Plasmas **5**, 743 (1998).
[11] A. Cardinali, R. Cesario, and F. De Marco, *Proceedings of the 21st EPS Conference on Controlled Fusion and Plasma Physics*, edited by E. Joffrin, P. Platz, and P. E. Stott (EPS, Montpellier, France, 1994), Vol. 18B, part II, p. 968.
[12] R. Cesario *et al.*, in *2nd Europhysics Topical Conference on Radio Frequency Heating and Current Drive of Fusion Devices*, Brussels 1998, edited by J. Jaquinot, G. Van Oost, and R. R. Weynants (EPS, Petit-Lancy, 1998), Vol. 22A, p. 65, and references therein.
[13] R. Cesario *et al.*, Nucl. Fusion **38**, 31 (1998).
[14] T. H. Stix, *Waves in Plasmas* (AIP, New York, 1992).
[15] M. L. Apicella *et al.*, Nucl. Fusion **37**, 381 (1997).
[16] A. Cardinali, C. Castaldo, and R. Cesario, Phys. Plasmas **5**, 2871 (1998).
[17] A. M. Messiaen *et al.*, *Proceedings of the 26th EPS Conference on Controlled Fusion and Plasma Physics* (EPS, Maastricht, 1999), Vol. 23J, p. 605.
[18] G. Cenacchi and A. Taroni, in *Proceedings 8th Computational Physics, Computing in Plasma Physics*, Eibsee 1986 (EPS, Petit-Lancy, 1986), Vol. 10D, p. 57.
[19] F. Alladio *et al.*, *Proceedings of the 15th International Conference on Plasma Physics and Controlled Nuclear Fusion Research*, Seville 1994 (IAEA, Vienna, 1995), Vol. 2, p. 23.
[20] A. Cardinali *et al.*, Nucl. Fusion (to be published).
[21] M. N. Rosenbluth, Comments Plasma Phys. Controlled Fusion **2**, 125 (2000).